of the Th_2Ni_{17}-type structure decreases. This suggests that the degree of order of the Th_2Ni_{17}-type structures of Pr_2Co_{17} and Nd_2Co_{17} is lowest. Therefore, the Th_2Ni_{17}-type compounds for these R elements do not exist. The degree of order of the Th_2Ni_{17}-type structures of Ce_2Co_{17} and Ho_2Co_{17} is nearly ideal. One therefore gets only traces of the Th_2Zn_{17}-type structure even after prolonged annealing at lower temperatures. Dy_2Co_{17} appears to lie in between these two extreme cases. This is the reason that both modifications *i.e.* $Th_2Ni_{17} + Th_2Zn_{17}$-type, are obtained in almost equal proportions below 1200 °C.

Since those R elements, studied in this work are uniformly distributed throughout the whole rare-earth series, the results obtained for their A_2B_{17} compounds can generally be applied to all the R_2Co_{17} compounds (Fig. 1).

Buschow (1966) and Givord, Givord & Lemaire (1972) have explained the polymorphism of R_2Co_{17} in terms of the radii ratios of R and Co atoms. No doubt the atomic radii of R and Co atoms are important factors in the formation of R_2Co_{17}. However, the atomic ratio model alone cannot explain the polymorphism of R_2Co_{17} over the rare-earth series and the degree of order of R_2Co_{17} of the Th_2Ni_{17}-type structure.

In our opinion, the valence-electron concentration and the electron-spatial correlation play a deciding role in the stabilization of one or more of the polymorphic forms of R_2Co_{17} for a particular R element at a particular temperature.

References

OSTERTAG, W. & STRNAT, K. J. (1965). *Rare-Earth Cobalt Compounds with the* A_2B_{17} *Structure*, AFML Report.

BOUCHET, G., LAFOREST, J., LEMAIRE, R. & SCHWEIZER, J. (1966). *C.R. Acad. Sci. Paris*, 262, 1-4.

BUSCHOW, K. H. J. (1966). *J. Less-Common Metals*, 11, 204-208.

LEMAIRE, R. (1966). *Kobalt*, 33, 175-184.

GIVORD, D., GIVORD, F. & LEMAIRE, R. (1972). *J. Less-Common Metals*, 29, 389-396.

GIVORD, D., LEMAIRE, R. & MOREAU, E. (1972). *J. Less-Common Metals*, 29, 361-369.

KHAN, Y. & MUELLER, B. (1973). *J. Less-Common Metals*, 32, 37-43.

FLORIO, J. V., BAENZIGER, N. C. & RUNDLE, R. E. (1956). *Acta Cryst.* 9, 367-372.

LIPSON, H. (1950). *Prog. Metal Phys.* 2, 1-100.

STOLOFF, N. S. & DAVIES, R. G. (1966). *Prog. Metal Phys.* 13, 3-6.

BARRETT, C. S. & MASSALSKI, T. B. (1966). *Structure of Metals*, 3rd ed., pp. 270-275. New York: McGraw-Hill.

MAKAROV, E. S. & VINOGRADOV, S. I. (1956). *Sov. Phys. Crystallogr.* 1, 499-505.

PEARSON, W. B. (1972). *The Crystal Chemistry and Physics of Metals and Alloys*, pp. 643-48 and 16-18. New York: Wiley.

BUSCHOW, K. H. J. & VAN DER GOOT, A. S. (1971). *Acta Cryst.* B27, 1085-1088.

Crystal and Molecular Structure of 1,2,3,4,5,6,7,8-Octaethylporphinatodichlorotin(IV) Nitromethane Solvate

BY DAVID L. CULLEN AND E. F. MEYER, JR

Department of Biochemistry & Biophysics, Texas Agricultural Experiment Station, Texas A&M University, College Station, Texas 77843, U.S.A.

The structure of 1,2,3,4,5,6,7,8-octaethylporphinatodichlorotin(IV) has been determined from three-dimensional X-ray counter data. The compound crystallizes in the monoclinic space group $P2_1/a$ with a unit cell of $a = 16.571$ (5), $b = 15.173$ (5), $c = 8.231$ (4) Å, $\beta = 101.12$ (4)°. There are two molecules in the unit cell. The observed and calculated densities are 1.35 (2) and 1.38 g cm^{-3}. The structure was solved by Fourier methods and refined by least-squares techniques to a final conventional R index of 0.054 (based on F) for the 2541 reflections having $F^2 > 3\sigma(F^2)$. The metalloporphyrin is a distorted octahedral complex with chlorine atoms at the apices. There are two disordered solvent molecules of nitromethane per formula unit. The Sn–N bond lengths are 2.081 (5) and 2.083 (4) Å. These are quite long for metal-nitrogen distances in porphyrins, but very short compared to normal Sn–N bond distances. The Sn–Cl distance is 2.453 (2) Å. The macrocycle is planar with a macrocyclic angle between adjacent planes of 0.4°. Comparisons with other tin(IV) complexes show many similarities, but some striking differences, especially when *meso*-substituted porphyrins are considered.

Introduction

Recently there has been some interest in the structures of macrocyclic complexes of tin, both in the +2

and +4 oxidation states. These have exhibited a variety of coordination geometries including octahedral (Collins, Scheidt & Hoard, 1972; Cullen & Meyer, 1971a; Rodgers & Osborn, 1971), a four-coordinate phthalo-

cyanine complex of tin(II) in which the metal ion lies considerably out of the plane of the macrocycle (Friedel, Hoskins, Martin & Mason, 1970), and an unusual eight-coordinate complex with phthalocyanine which has a sandwich-type structure (Bennett, Broberg & Baenziger, 1973). The structure of octaethylporphinatodichlorotin(IV) nitromethane solvate, Cl_2SnOEP, was reported earlier (Cullen & Meyer, 1971a). These results were based on fairly low-order data. This structure has now been fully refined using higher-order data. It provides an excellent comparison with the other tin macrocyclic complexes, particularly the structure of $\alpha,\beta,\gamma,\delta$-tetraphenylporphinatodichlorotin(IV), Cl_2SnTPP, which was determined with an unusually high degree of accuracy by Collins et al. (1972). The macrocycles differ in that tetraphenylporphyrin is substituted at the four meso carbon atom positions while octaethylporphyrin has substitutents at the eight β carbon atoms of the pyrrole ring. Although both macrocycles are synthetic the latter corresponds more closely to naturally occurring porphyrins. Thus, a study of similar complexes of the two differently substituted porphyrins provides insights into the effect of substitution on the geometry of the macrocycle.

Experimental

Samples of 1,2,3,4,5,6,7,8-octaethylporphinatodichlorotin(IV) $(C_{36}H_{44}N_4SnCl_2)$ were supplied by Dr David Dolphin of Harvard University. Reddish violet rods, elongated along c and bounded by $\{110\}$ were crystallized from a mixture of benzene, dichloromethane, and nitromethane. The crystal used for intensity measurements was cut from a larger crystal and mounted (Meyer, 1973) in a glass capillary. The cleavage faces of the crystal are best described as the $(01\bar{1})$ and the $(5\bar{2}6)$. The approximate dimensions of the crystal are 0·21 and 0·23 mm in the direction of [110] and [1$\bar{1}$0] respectively, while the mean distance along the long direction of the rod is 0·39 mm.

Cell data are summarized in Table 1. Cell dimensions were determined by least-squares calculations, minimizing the differences between observed and calculated 2θ values for 12 reflections. The ambient temperature was 20 °C. The density was measured in an aqueous potassium iodide solution. From the density measurements and eventual solution of the structure, it became apparent that there were two nitromethane solvent molecules per formula unit.

Table 1. *Cell data for* $Cl_2SnOEP.2CH_3NO_2$

(Estimated standard deviations in parentheses)

$a = 16·571$ (5) Å	Space group $P2_1/a$
$b = 15·173$ (5)	$Z = 2$
$c = 8·231$ (4)	M.W. 848·3
$\beta = 101·12$ (4)°	$D_c = 1·38$ g cm^{-3}
$V = 2030·1$ Å^3	$D_m = 1·35$ (2) g cm^{-3}
$\mu = 8·11$ cm^{-1}	
Systematic absences	$h0l$ (h odd); $0k0$ (k odd)

Intensity data were collected on a Datex-Syntex automated four-circle diffractometer using Mo $K\alpha$ radiation ($\lambda = 0·71069$ Å). The radiation was monochromated by pyrolytic graphite. The data were collected by the θ–2θ scan method, monitoring the intensity scale by remeasuring a group of five standard reflections periodically. The intensities of these standard reflections varied by $\pm 3\%$ with no systematic trend. The variations were attributed to statistical fluctuations and not to crystal decomposition or other systematic errors, and no corrections were made. The scan rate was 3 deg min^{-1}. The scan range was calculated from the relationship: range (°) = 1·94° sin θ + 1·34°.

3713 independent reflections were measured out to a sin θ/λ of 0·595 or 25 °θ. The F_o^2 values were calculated by the relationship $F_o^2 = Lp [S - T_s/2T_b(B1 + B2)]$. S is the scan count measured for time T_s and $B1$ and $B2$ are the backgrounds each measured for a time T_b of 20 sec. Lorentz and polarization factors, Lp, were applied assuming an ideally imperfect monochromator.

2541 reflections had F_o^2 greater than $3\sigma(F_o^2)$ and were used for the analysis. This corresponds to a data/parameter ratio of 11·7 if hydrogen atoms are not included or 8·3 if they are included. The standard deviation $\sigma(F_o^2)$ was defined in terms of the statistical variances of the count as $\sigma(F_o^2) = [\sigma^2(\text{count}) + (0·05F_o^2)^2]^{1/2}$, where $\sigma^2(\text{count}) = Lp [S + (T_s/2T_b)^2(B1 + B2)]$.

The data were corrected for absorption by means of a Gaussian integration method, even though the range of transmission coefficients of 0·83 to 0·88 was fairly narrow. When the data were examined by the method of Housty & Clastre (1957), no reflections appeared to be affected by extinction, and no correction was therefore made.

Determination and refinement of the structure

Because there are two molecules in the unit cell of space group $P2_1/a$, the tin atom is required to be at a center of symmetry, selected to be at $\frac{1}{2},\frac{1}{2},0$. From a series of Fourier and difference maps the positions of the rest of the 22 independent non-hydrogen atoms in the porphyrin moiety were found. The positions of the 22 hydrogen atoms in the asymmetric unit were located in difference syntheses calculated after initial least-squares refinement of the non-hydrogen atoms.

The difference maps also clearly indicated the presence of a disordered solvent molecule. This appeared to be a planar molecule containing four atoms of approximately the same atomic number. The disorder appeared to be such that there were two different orientations with a common central atom. Of the solvents used in the preparation and recrystallization, it seemed most likely that the solvent molecule was nitromethane. Because of the disorder it was not possible to identify which were carbon or oxygen atoms, so in subsequent refinements, all the atoms of the solvent molecule were called nitrogen atoms and were given isotropic tem-

perature factors of 10·0 Å². All but the central atom were given half occupancy factors.

Block-diagonal and finally full-matrix methods were used in the least-squares refinement. The function

minimized was $\sum w(F_o^2 - F_c^2)^2$, where $w = 1/\sigma^2(F_o^2)$. Initially isotropic temperature factors were used. In the final refinements, all atoms were refined assuming anisotropic thermal motion except the hydrogen atoms

Table 2. *Observed and calculated structure factors*

The columns are k, l, F_{obs}^2, F_{cal}^2.

and those in the solvent molecule, which were assumed to have isotropic thermal motion. The temperature factors of the solvent molecule atoms were not refined. Because of space limitations the parameters had to be refined in two blocks during the full-matrix least-squares refinement. In one block all non-hydrogen atoms except for those of the solvent molecule were refined. In the other block the tin atom, the solvent molecule atoms, the hydrogen atoms and the carbon atoms to which they were bonded, were refined. The refinement converged with $R = \sum|F_o^2 - |F_c|^2|/\sum F_o^2 = 0.094$ and $R_w = (\sum w|F_o^2 - |F_c|^2|^2/\sum wF_o^4)^{1/2} = 0.132$. The conventional R value based on F is 0.054 while the R_w value is 0.063 $[R = \sum|F_o - |F_c||/\sum F_o$ and $R_w = (\sum w|F_o - |F_c||^2/\sum wF_o^2)^{1/2}]$. If those reflections with $F^2 < 3\sigma(F^2)$ are included, R (based on F^2) is 0.100.

A correction for anomalous dispersion was made for the tin atom ($\Delta f' = -0.6$ to -0.7, $\Delta f'' = 1.9$ to 1.7) and for the chlorine atom ($\Delta f' = 0.1$, $\Delta f'' = 0.2$) (*International Tables for X-ray Crystallography*, 1962). Scattering factors from *International Tables for X-ray Crystallography* (1973) were used. The tin and chlorine atoms were assumed to be in the zero ionization state.

In the last cycle all shifts were less than one standard deviation except for some of the parameters of the solvent molecule atoms. Because these shifts were only slightly above one standard deviation, further refinement seemed unwarranted. Also in the final refinement, the position of H(11) which had been refining to physically unreasonable values was held fixed at its calculated position. The final value of the standard deviation

of an observation of unit weight was 1.64. In the final difference synthesis there were three peaks ranging from 0.9 to 1.2 eÅ⁻³. These were all close to the tin atom position and were not considered of physical significance. No other peak was higher than 0.55 eÅ⁻³. These three largest peaks are probably due to inaccuracies in the low-order data since they were not present on a difference synthesis calculated using only contributions from reflections having $\sin\theta/\lambda \geq 0.30$.

The following computer programs were used: *LSLAT* (cell parameter refinement); *DATAPH* (absorption corrections), (P. Coppens, unpublished); *LINUS* (modification of the Busing, Martin & Levy (1962) *ORFLS* least-squares program); *BDLR4* (block-diagonal least-squares program); *JIMDAP* (version of the Zalkin Fourier summation program); *ORFFE* (function and error program, Busing, Martin & Levy, 1964); *ORTEP* (thermal ellipsoid plot program of Johnson, 1965), and *HOW* (molecular geometry program). In addition several local data handling programs were used. Extensive use was made of the interactive color TV raster display in this laboratory for which routines have been written by Sparks (unpublished) and extensively modified locally (Willoughby & Meyer, 1973; Morimoto & Meyer, 1973).

The observed and calculated squared structure factors are listed in Table 2. The final positional and thermal parameters from the last cycle of refinement are given in Table 3, while the root-mean-square components of thermal displacement along the principal axes of thermal ellipsoids are given in Table 4.

Table 3. *Fractional coordinates and thermal motion parameters derived from the least-squares refinement*

In this and subsequent tables estimated standard deviations are in parentheses. Parameters with no standard deviations were fixed by symmetry or were not refined. The Debye–Waller factor is defined as:

$$T = \exp[-2\pi^2 \sum_i \sum_j a_i^* a_j^* h_i h_j U_{ij}]$$

The values for U have been multiplied by 10^4. For the hydrogen and solvent molecule atoms, isotropic B's are defined by $\exp[-B(\sin^2\theta)/\lambda^2]$. These have been multiplied by 10.

	x	y	z	U(11)	U(22)	U(33)	U(12)	U(13)	U(23)
Sn	0.5000	0.5000	0.0000	288 (2)	403 (3)	259 (2)	−55 (3)	−60 (1)	33 (3)
Cl	0.4363 (1)	0.6284 (1)	0.1053 (2)	535 (11)	567 (10)	480 (9)	45 (8)	−22 (8)	−15 (8)
N(1)	0.4010 (2)	0.4904 (3)	−0.1977 (5)	330 (24)	414 (29)	317 (23)	−86 (24)	−17 (19)	−12 (23)
N(2)	0.4399 (2)	0.4171 (3)	0.1398 (5)	322 (27)	404 (28)	292 (25)	−84 (23)	− 6 (21)	45 (22)
C(1)	0.3964 (3)	0.5300 (3)	−0.3507 (7)	341 (32)	386 (33)	294 (31)	51 (25)	−25 (25)	7 (24)
C(2)	0.3175 (3)	0.5060 (4)	−0.4515 (6)	361 (28)	392 (31)	289 (26)	65 (31)	−71 (22)	−59 (30)
C(3)	0.2776 (3)	0.4534 (3)	−0.3582 (7)	296 (31)	376 (33)	324 (30)	6 (26)	−70 (25)	−41 (26)
C(4)	0.3294 (3)	0.4435 (3)	−0.1998 (6)	298 (30)	378 (35)	332 (31)	−42 (26)	−47 (25)	23 (26)
C(5)	0.3136 (3)	0.3938 (3)	−0.0667 (7)	316 (32)	436 (36)	399 (34)	−78 (27)	−46 (26)	33 (28)
C(6)	0.3627 (3)	0.3811 (3)	0.0887 (6)	294 (33)	361 (33)	366 (32)	−32 (25)	−45 (25)	49 (26)
C(7)	0.3431 (3)	0.3293 (3)	0.2222 (7)	341 (32)	370 (33)	406 (32)	−30 (26)	55 (26)	− 5 (27)
C(8)	0.4079 (3)	0.3369 (3)	0.3534 (7)	374 (33)	342 (33)	367 (33)	18 (26)	37 (27)	27 (26)
C(9)	0.4682 (3)	0.3924 (3)	0.3012 (6)	347 (33)	427 (37)	273 (30)	25 (27)	−37 (25)	43 (26)
C(10)	0.4565 (3)	0.5820 (3)	−0.3940 (6)	422 (34)	376 (32)	235 (28)	1 (27)	−10 (26)	55 (25)
C(11)	0.2891 (4)	0.5392 (4)	−0.6264 (7)	464 (38)	563 (38)	289 (32)	7 (32)	−128 (28)	− 2 (29)
C(12)	0.2562 (5)	0.6313 (5)	−0.6324 (9)	896 (63)	747 (55)	567 (46)	284 (48)	−46 (43)	169 (42)
C(13)	0.1937 (3)	0.4135 (4)	−0.4089 (7)	399 (37)	549 (41)	411 (36)	−94 (31)	−120 (29)	30 (31)
C(14)	0.1265 (5)	0.4710 (6)	−0.3747 (17)	394 (45)	932 (71)	1404 (117)	−80 (41)	42 (61)	−165 (71)
C(15)	0.2651 (4)	0.2784 (5)	0.2149 (8)	452 (42)	642 (48)	511 (42)	−136 (36)	−53 (34)	199 (37)
C(16)	0.2709 (5)	0.1860 (6)	0.1550 (12)	815 (63)	776 (64)	1136 (76)	−335 (50)	−22 (57)	−206 (56)
C(17)	0.4179 (4)	0.2945 (4)	0.5184 (7)	490 (39)	504 (40)	341 (33)	−74 (31)	15 (29)	35 (29)
C(18)	0.4729 (5)	0.2163 (4)	0.5396 (8)	940 (62)	519 (46)	510 (45)	60 (42)	−55 (40)	198 (35)

Table 3 (cont.)

	x	y	z	B
N(3)	0·0498 (7)	0·3933 (8)	0·0901 (14)	100
N(4)	−0·033 (1)	0·350 (1)	0·003 (2)	100
N(5)	0·106 (1)	0·442 (1)	0·073 (2)	100
N(6)	0·046 (1)	0·423 (1)	0·234 (2)	100
N(7)	0·085 (1)	0·384 (1)	−0·043 (2)	100
N(8)	0·059 (1)	0·480 (1)	0·155 (2)	100
N(9)	0·012 (1)	0·314 (1)	0·086 (2)	100
H(1)	0·265 (3)	0·367 (4)	−0·085 (7)	39 (14)
H(2)	0·448 (2)	0·598 (2)	−0·489 (5)	10 (8)
H(3)	0·258 (4)	0·507 (4)	−0·672 (9)	39 (16)
H(4)	0·333 (3)	0·535 (3)	−0·692 (7)	35 (13)
H(5)	0·304 (5)	0·676 (5)	−0·592 (10)	80 (22)
H(6)	0·208 (6)	0·632 (6)	−0·559 (12)	67 (30)
H(7)	0·238 (4)	0·640 (5)	−0·741 (10)	61 (20)
H(8)	0·178 (3)	0·408 (3)	−0·518 (8)	27 (13)
H(9)	0·187 (4)	0·356 (5)	−0·370 (9)	73 (20)
H(10)	0·120 (6)	0·514 (7)	−0·430 (14)	87 (37)
H(11)	0·138	0·486	−0·253	80
H(12)	0·072 (5)	0·452 (5)	−0·406 (9)	62 (17)
H(13)	0·224 (4)	0·314 (4)	0·150 (10)	61 (19)
H(14)	0·256 (3)	0·273 (3)	0·323 (8)	30 (14)
H(15)	0·323 (7)	0·158 (7)	0·219 (15)	116 (38)
H(16)	0·291 (5)	0·179 (5)	0·045 (11)	59 (23)
H(17)	0·224 (7)	0·161 (7)	0·151 (14)	109 (33)
H(18)	0·367 (4)	0·284 (4)	0·536 (7)	39 (16)
H(19)	0·432 (4)	0·329 (4)	0·589 (8)	43 (17)
H(20)	0·459 (4)	0·175 (4)	0·465 (9)	44 (18)
H(21)	0·529 (6)	0·222 (6)	0·518 (11)	84 (27)
H(22)	0·472 (4)	0·189 (4)	0·616 (8)	35 (16)

Table 4. Root-mean-square amplitudes of vibration (Å) of the principal axes of thermal ellipsoids

	Axis 1	Axis 2	Axis 2
Sn	0·133 (1)	0·184 (1)	0·219 (1)
Cl	0·201 (2)	0·234 (2)	0·261 (2)
N(1)	0·152 (8)	0·193 (7)	0·221 (7)
N(2)	0·158 (8)	0·171 (8)	0·224 (7)
C(1)	0·153 (10)	0·192 (8)	0·213 (8)
C(2)	0·144 (9)	0·183 (9)	0·236 (9)
C(3)	0·141 (10)	0·191 (9)	0·221 (8)
C(4)	0·149 (10)	0·188 (9)	0·219 (8)
C(5)	0·156 (10)	0·198 (9)	0·238 (8)
C(6)	0·152 (10)	0·182 (9)	0·224 (8)
C(7)	0·179 (9)	0·197 (9)	0·203 (8)
C(8)	0·177 (9)	0·193 (9)	0·204 (8)
C(9)	0·145 (10)	0·208 (9)	0·211 (8)
C(10)	0·143 (10)	0·196 (9)	0·218 (8)
C(11)	0·138 (11)	0·237 (8)	0·254 (8)
C(12)	0·185 (11)	0·283 (10)	0·338 (11)
C(13)	0·152 (11)	0·223 (9)	0·267 (9)
C(14)	0·195 (12)	0·301 (12)	0·387 (15)
C(15)	0·188 (11)	0·197 (10)	0·304 (9)
C(16)	0·198 (12)	0·335 (12)	0·360 (11)
C(17)	0·181 (10)	0·207 (9)	0·247 (9)
C(18)	0·171 (11)	0·263 (10)	0·326 (9)

Discussion

A drawing of the structure of 1,2,3,4,5,6,7,8-octaethyl-porphinatodichlorotin(IV) (Cl$_2$SnOEP) is shown in Fig. 1. Fig. 2 shows the averaged bond lengths and angles and shows the nomenclature for various types of carbon atoms which will be used in the subsequent discussion. The metalloporphyrin is a centrosymmetric distorted octahedral complex with the chlorine atoms located at apical positions. The tin atom is located in the plane of the macrocycle. This supports the published interpretation of the spectra of various Sn(IV) porphyrins and phthalocyanine complexes (O'Rourke & Curran, 1970). The two Sn–N distances are 2·081 (5) and 2·083 (4) Å. Within experimental error, the bond angles around the tin atom are 90°. Bond lengths and angles for this complex are listed in Table 5.

Table 5. Bond lengths and angles

Some non-bonding distances of interest are also given.

Sn —Cl	2·453 (2) Å	Cl——Sn —N(1)	90·2 (1)°
Sn —N(1)	2·081 (5)	Cl——Sn —N(2)	90·0 (1)
Sn —N(2)	2·083 (5)	N(1)-Sn —N(2)	90·1 (2)
N(1)–C(1)	1·384 (7)	Sn —N(1)–C(1)	125·3 (3)
N(1)–C(4)	1·381 (7)	Sn —N(1)–C(4)	126·3 (3)
N(2)–C(6)	1·379 (7)		
N(2)–C(9)	1·372 (7)	Sn —N(2)–C(6)	125·8 (3)
C(1)–C(2)	1·452 (8)	Sn —N(2)–C(9)	126·1 (3)
C(1)–C(10)	1·371 (8)	C(1)–N(1)–C(4)	108·4 (5)
C(2)–C(3)	1·364 (8)	C(6)–N(2)–C(9)	108·1 (5)
C(2)–C(11)	1·512 (8)	N(1)–C(1)–C(2)	107·2 (5)
C(3)–C(4)	1·423 (8)	N(1)–C(1)–C(10)	124·8 (5)
C(3)–C(13)	1·500 (8)	C(2)–C(1)–C(10)	127·9 (6)
C(4)–C(5)	1·395 (8)	C(1)–C(2)–C(3)	107·8 (5)
C(5)–C(6)	1·390 (8)	C(1)–C(2)–C(11)	122·7 (6)
C(6)–C(7)	1·439 (8)	C(3)–C(2)–C(11)	129·4 (5)
C(7)–C(8)	1·372 (8)	C(2)–C(3)–C(4)	107·8 (5)
C(7)–C(15)	1·497 (9)	C(2)–C(3)–C(13)	127·1 (5)
C(8)–C(9)	1·435 (8)	C(4)–C(3)–C(13)	125·1 (5)
C(8)–C(17)	1·481 (8)	C(3)–C(4)–C(5)	127·2 (5)
C(9)–C(10)′	1·387 (8)	N(1)–C(4)–C(3)	108·7 (5)
C(11)–C(12)	1·498 (10)	N(1)–C(4)–C(5)	124·0 (5)
	1·526 (12)*		
C(13)–C(14)	1·484 (11)	C(4)–C(5)–C(6)	129·2 (6)
	1·527 (12)*		
C(15)–C(16)	1·495 (12)	N(2)–C(6)–C(5)	124·7 (5)
	1·534 (12)*		
C(17)–C(18)	1·486 (10)	N(2)–C(6)–C(7)	108·4 (5)
	1·507 (10)*		
Sn —C(5)	3·432 (6)	C(5) –C(6)—C(7)	126·9 (6)
Sn —C(10)	3·417 (6)	C(6) –C(7)—C(8)	107·3 (5)
N(1)–N(2)	2·946 (6)	C(6) –C(7)—C(15)	124·9 (6)
N(1)–N(2)′	2·943 (6)	C(8) –C(7)—C(15)	127·8 (5)
N(3)–N(4)	1·56 (2)	C(7) –C(8)—C(9)	107·3 (5)
N(3)–N(5)	1·22 (2)	C(7) –C(8)—C(17)	128·0 (5)
N(3)–N(6)	1·28 (2)	C(9) –C(8)—C(17)	124·7 (5)
N(3)–N(7)	1·34 (2)	N(2) –C(9)—C(8)	108·8 (5)
N(3)–N(8)	1·42 (2)	N(2) –C(9)—C(10)′	124·0 (5)
N(3)–N(9)	1·35 (2)	C(8) –C(9)—C(10)′	127·1 (5)
		C(9)′–C(10)–C(1)	129·8 (6)
		C(2) –C(11)–C(12)	112·7 (6)
		C(3) –C(13)–C(14)	113·5 (6)
		C(3) –C(15)–C(6)	112·8 (7)
		C(3) –C(17)–C(18)	114·3 (6)
		N(4) –N(3)—N(5)	145· (2)
		N(4) –N(3)—N(6)	112· (2)
		N(5) –N(3)—N(6)	94· (2)
		N(7) –N(3)—N(8)	112· (2)
		N(7) –N(3)—N(9)	99· (2)
		N(8) –N(3)—N(9)	148· (2)

Symmetry code
′   1−x   1−y   −z
* Corrected for thermal motion.

Two features distinguish the tin porphyrins. One is the length of the tin–pyrrole nitrogen atom distances and the other is the planarity of the metal and macrocyclic ligand.

The length of normal Sn–N covalent bonds is *ca.* 2·18 Å, as was found, for example, in the structure of 2,2'-bipyridyltetrafluorotin(IV) (Adley, Bird, Frazer & Onyszchuk, 1972). On the other hand Collins & Hoard (1970) have estimated the normal size in the 'hole' of a porphyrin to be 2·01 Å. Thus the average 2·081 (2) Å distance here reported as well as the significantly longer Sn–N distance of 2·098 (2) Å in Cl_2SnTPP represents a

compromise between the two tendencies and results in a considerable expansion of the porphinato core. In the analogous dichlorophthalocyanotin(IV) (Cl_2SnPc) (Rodgers & Osborn, 1971), the average Sn–N distance is shorter yet, 2·050 (3) Å, and can be attributed to the geometry of the phthalocyanine macrocycle which reduces the size of the central hole. A comparison of several macrocyclic tin complexes is given in Table 6.

Table 6. *Some averaged bond lengths and angles for tin macrocylic complexes*

Figures in parentheses are root-mean-square standard deviations of least significant figure when there is more than one contribution to the average, otherwise estimated standard deviation is given.

	$Cl_2Sn(IV)OEP^a$	$Cl_2Sn(IV)TPP^b$	$Cl_2Sn(IV)Pc^c$	$Sn(IV)Pc_2^d$	$Sn(II)Pc^e$
Sn–Cl	2·453 (2) Å	2·420 (1)	2·448 (1)		
Sn–N	2·082 (2)	2·098 (2)	2·051 (2)	2·35 (2)	2·25 (2)
N–C_a	1·379 (5)	1·370 (2)	1·378 (2)	1·38 (3)	1·373 (8)
C_a–C_m	1·386 (10)	1·407 (2)			
C_a–C_b	1·437 (12)	1·446 (1)	1·454 (6)	1·47 (3)	1·456 (3)
C_a–C_b	1·368 (5)	1·380 (3)	1·405 (3)	1·39 (3)	1·391 (8)
C_m–Sn	3·424 (10)	3·469 (2)			
N–N	2·944 (2)	2·967 (2)			
Cl–Sn–N	90·1 (1)	90·0			
N–Sn–N	90·0 (1)	90·0	90·1		
Sn–N–C_a	125·9 (4)	125·4 (2)	123·8 (5)		
C_a–N–C_a	108·2 (2)	109·2 (2)	111·4 (2)	108 (2)	108·2 (7)
N–C_a–C_b	108·3 (7)	108·3 (2)	106·8 (2)	108 (2)	108·2 (7)
N–C_a–C_m	124·4 (4)	126·4 (2)			
C_b–C_a–C_m	127·3 (4)	125·4 (2)			
C_a–C_b–C_b	107·6 (3)	107·2 (2)	107·5 (4)	109 (3)	106·6 (3)
C_a–C_m–C_a	129·5 (4)	126·3 (2)			

(a) This work; (b) Collins, Scheidt & Hoard (1972); (c) Rodgers & Osborn (1971); (d) Bennett, Broberg & Baenziger (1973); (e) Friedel, Hoskins, Martin & Mason (1970).
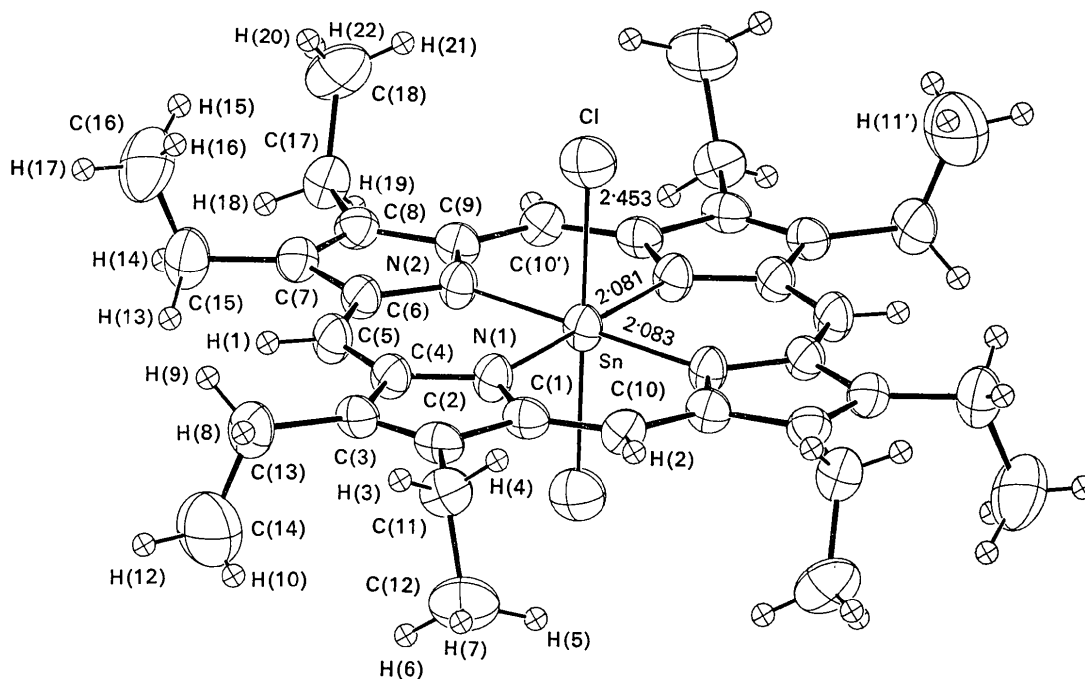

Fig. 1. *ORTEP* drawing of 1,2,3,4,5,6,7,8-octaethylporphinatodichlorotin(IV) showing numbering scheme and tin–ligand atom distances. Atoms not labelled are centrosymmetrically related. The thermal ellipsoids are drawn for 50 % probability, except for those of the hydrogen atoms, which are not drawn to scale.

The Sn–Cl distance, 2·453 (2) Å, is significantly longer in Cl_2SnOEP than in Cl_2SnTPP. Collins, Scheidt & Hoard (1972) have postulated that because the packing of the six ligand atoms around the tin atom is so tight, the severe shortening found for the equatorial bonds would cause a lengthening of the axial bonds. Since the equatorial bonds in Cl_2SnOEP are shorter than those in Cl_2SnTPP, the axial bonds would be longer. This is supported by the observation
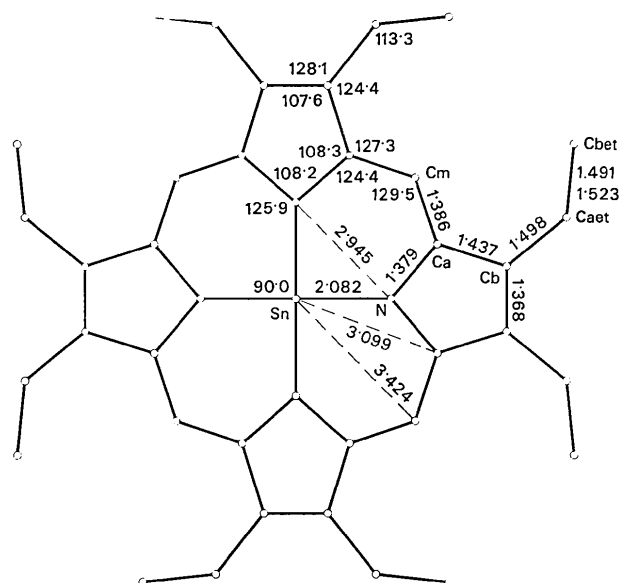

Fig. 2. Schematic drawing of the octaethylporphinatotin(IV) macrocycle showing averaged bond lengths in Å and angles in degrees. The two values for the Caet–Cbet bonds are the uncorrected distance (upper value) and the distance corrected for thermal motion (lower value). Also shown is the notation for different types of carbon atoms.
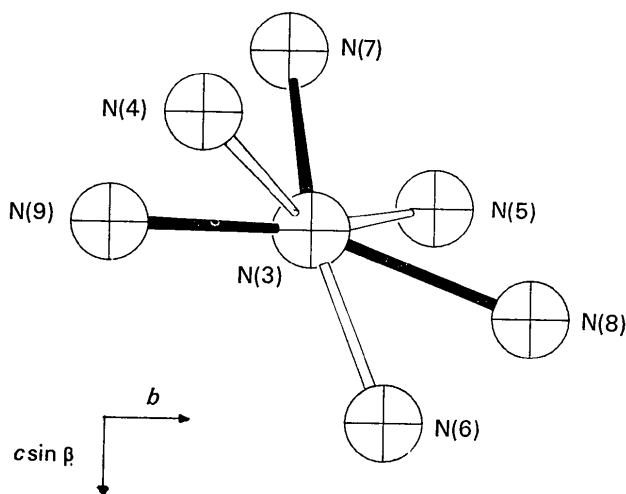

Fig. 3. Model chosen to describe disordered solvent molecule. Open bonds indicate orientation 1, solid bonds indicate orientation 2. View is projection onto b^*c^* plane.

that in either case the Sn–Cl distance is considerably longer than most previously reported Sn–Cl bonds. For example the bond distance in tin(IV) chloride glutaronitrile (Barnhart, Caughlan & Ul-Haque, 1968) is 2·35 Å. It is interesting to note that the Sn–Cl bond distance in Cl_2SnPc is the same within experimental error as Cl_2SnOEP even though the phthalocyanine complex has significantly shorter equatorial bonds.

Several differences between Cl_2SnOEP and Cl_2SnTPP may be noted in the averaged bond lengths and angles in Table 6. Of the differences in bond lengths, those between C_a–C_m and the C_b–C_b distances are only possibly significant, while the differences in the Sn–C_m distances are definitely significant. In the latter case these distances are shorter in Cl_2SnOEP. A similar effect was found in the structural determinations of $\alpha,\beta,\gamma,\delta$-tetra(4-pyridyl)porphinatomonopyridinezinc(II) (Collins & Hoard, 1970) and octaethylporphinato-monopyridinezinc(II) (Cullen & Meyer, 1971b), both five-coordinate complexes with the metal atom out of the plane of the macrocycle. In these the center–methine carbon atom distances are 3·448 and 3·392 Å, respectively. Similarly in the recent determination of the structure of the free base of octaethylporphyrin (Lauher & Ibers, 1973) the center–methine carbon atom distance is 3·42 Å, while in various meso-substituted free base porphyrins this distance varies from 3·44–3·45 Å (Codding & Tulinsky, 1972; Silvers & Tulinsky, 1967). In the tetragonal form of tetraphenylporphyrin (Hamor, Hamor & Hoard, 1964) this distance is the same as in octaethylporphyrin and as in porphine itself (Chen & Tulinsky, 1972).

It would thus appear that for porphyrins which are unsubstituted at the meso-position, the methine carbon atom can be drawn in closer to the center. This causes a larger C_a–C_m–C_a angle (129·5° in Cl_2SnOEP as compared to 126·4° in Cl_2SnTPP). This also results in a closing of the N–C_a–C_m angles and an opening of the C_b–C_m–C_a angles for Cl_2SnOEP as compared to Cl_2SnTPP. The average Sn–C_a distance is the same in both complexes, 3·10 Å. A similar opening of the C_a–C_m–C_a angle is observed when the structures of octaethylporphinatomonopyridinezinc(II) and the free base of octaethylporphyrin are compared with their meso-substituted analogs.

In their comparison of pyrrole-substituted and meso-substituted free base porphyrins Lauher & Ibers (1973) have noted that the carbon–carbon bonds closest to the site of substitution are lengthened. However within experimental error this does not seem to be the case when Cl_2SnTPP and Cl_2SnOEP are compared. The C_a–C_m distance is shorter in Cl_2SnOEP than in Cl_2SnTPP, but the C_b–C_b distance in the former is actually significantly shorter, whereas it might be expected to be longer.

The values for the terminal C–C bonds as originally calculated are unusually short. This is probably due to thermal shortening. When these bond distances were corrected for thermal motion effects, assuming a

'riding' model, more reasonable values were obtained. Both values are given in Table 5.

The hydrogen atoms of the ethyl groups show the expected staggered configuration. Because of the presence of highly scattering atoms like tin and chlorine, the standard deviations on bond lengths and angles involving hydrogen atoms are fairly large. The problem is compounded further by the effect of the disordered solvent molecule on the low-order data. The estimated standard deviation for C–H bonds is 0·05–0·08 Å; for C–C–H angles it is 3–5°; for H–C–H angles it is 5–6°.

On resonance grounds the porphyrin macrocycle is predicted to be planar. Yet, for most so-called planar porphyrins the angle between planes of adjacent pyrrole groups is of the order of 3–5°. The greatest deviation from planarity thus far reported for a metallo-porphyrin is the tetragonal form of nickel(II)octa-ethylporphyrin (NiOEP) (Meyer, 1972). where the angle between planes of adjacent pyrrole groups is 32·8°. The macrocycle in both Cl_2SnOEP and Cl_2SnTPP is unusually planar. In the latter complex all of the atoms of the macrocycle lie in a mirror plane, hence the molecule is constrained to be planar and have at least C_{4h} symmetry. In the case of Cl_2SnOEP the only required crystallographic symmetry is a center of inversion, but the angle between adjacent rings is 0·4.° Deviations from the least-squares plane passing through the metal and macrocyclic atoms are shown in Table 7; the greatest deviation is 0·02 Å for N(2).

In the case of the tetragonal form of NiOEP, the metal–nitrogen atom bond length is unusually short, 1·929 (3) Å. In order to attain this short bond length, the macrocycle distorts to an effectively D_{2d} symmetry. It would appear that the energies involved in this deformation are not large, because recently the structure of a triclinic form of NiOEP has been determined (Cullen & Meyer, 1973). This has a planar macrocycle and has a somewhat longer Ni–N bond length (1·96 Å) than the tetragonal form. Hoard (1972) has treated

Table 7. *Deviation* (Å) *from least-squares planes*

	Plane 1	Plane 2	Plane 3	Plane 4
Sn	0·011 Å	0·000	−0·009	0·032
N(1)	0·011	0·000	0·001	0·055
N(2)	−0·021	0·000	−0·059	−0·010
C(1)	−0·004	−0·033	−0·001	0·054
C(2)	−0·005	−0·027	0·001	0·066
C(3)	0·005	0·004	−0·001	0·070
C(4)	0·015	0·021	−0·001	0·063
C(5)	0·003	0·029	−0·026	0·039
C(6)	−0·009	0·024	−0·048	0·010
C(7)	−0·014	0·040	−0·067	−0·007
C(8)	0·008	0·062	−0·052	0·001
C(9)	0·011	0·045	−0·039	0·006
C(10)	−0·011	−0·060	0·001	0·048
C(11)	0·020	−0·017	0·040	0·109
C(13)	0·025	0·038	0·017	0·098
C(15)	−0·024	0·048	−0·084	−0·012
C(17)	−0·013	0·059	−0·087	−0·031

Plane 1: Macrocycle [Sn, N(1), N(2), C(1)–C(10)]
  $-8·15X + 12·19Y + 3·49Z = 2·0$
Plane 2: 4N [N(1), N(2), N(1)', N(2)']
  $-8·30X + 12·04Y + 3·58Z = 1·87$
Plane 3: Pyrrole ring 1 [N(1), C(1)–C(4)]
  $-8·12X + 12·26Y + 3·42Z = 2·08$
Plane 4: Pyrrole ring 2 [N(2), C(6)–C(9)]
  $-8·22X + 12·22Y + 3·41Z = 1·97$
Note: All planes are unweighted. X, Y, Z are in monoclinic fractional coordinates.

possible distortions from the idealized D_{4h} symmetry in a quantitative manner. He points out that while distortion to a D_{2d} symmetry is an effective way of removing strain when an undersized metal ion like Ni(II) is coordinated, a distortion to D_{2d} symmetry will not remove the strain caused by an oversized ion like Sn(IV). A distortion to C_{4v} symmetry which should theoretically remove the strain caused by an oversized ion is actually very inefficient for this purpose.

All three of the tin phthalocyanine complexes show distortions of the macrocycle from planarity. Both Cl_2SnPc and stannous phthalocyanine show a ruffling of the macrocycle, while in the eight-coordinate sand-
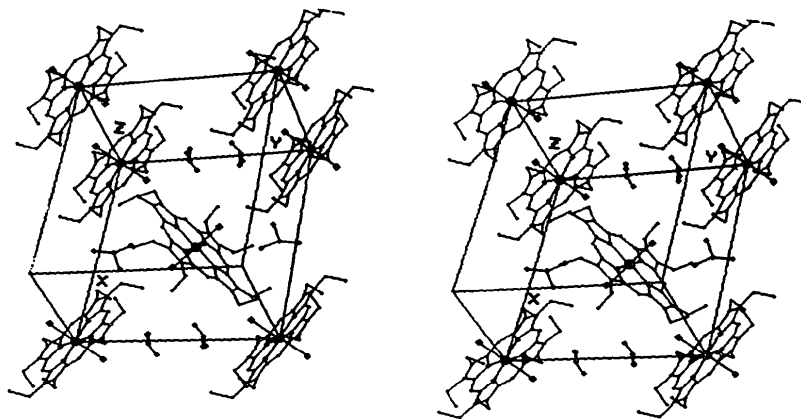

Fig. 4. Stereoview of packing in the unit cell. For clarity only two of the molecules related by a unit translation along z are shown. Only one orientation of the solvent molecule is shown at a given site. Those near $x = 0$ and $x = 1$ are in orientation 1. Those near $x = \frac{1}{2}$ are in orientation 2.

wich type complex bisphthalocyanotin(IV) the macrocycles do show a distortion to C_{4v} symmetry.

The solvent molecule, which is probably nitromethane, is highly disordered. The model which was chosen to describe it has two different orientations of the molecule which are not coplanar, as there is an angle of 39° between the least-squares planes of the two. N(3) is the central atom for both orientations. Bond lengths and angles for either orientation are not particularly good. They agree only roughly with those found for the nitromethane molecule of solvation in the structure determination of 2,2'-bipyridyltetra-fluorotin(IV) (Adley *et al.*, 1972). Fig. 3 shows the orientation of the solvent molecule for the model chosen. We appreciate the referee's suggestions as to the choice of the optimum configuration of the two molecules.

Fig. 4 is a packing diagram of Cl₂SnOEP. There are no unusually short contacts other than some with atoms in the solvent molecule. The shortest of these is 3·32 Å for N(6)–C(14). Considering the lack of accuracy in the positions of solvent molecule atoms, this may not be significant. The shortest intermolecular contact between atoms of the porphyrin is 3·50 Å. The closest contacts to the chlorine atom are 3·42 Å for N(9) and 3·82 Å for C(18).

References

ADLEY, A. D., BIRD, P. H., FRASER, A. R. & ONYSZCHUK, M. (1972). *Inorg. Chem.* **11**, 1402–1409.

BARNHART, D. M., CAUGHLAN, C. N. & UL-HAQUE, M. (1968). *Inorg. Chem.* **7**, 1135–1138.

BENNETT, W. E., BROBERG, D. E. & BAENZIGER, N. C. (1973). *Inorg. Chem.* **12**, 930–936.

BUSING, W. R., MARTIN, K. O. & LEVY, H. (1962). *ORFLS.* Report ORNL-TM-305, Oak Ridge National Laboratory Oak Ridge, Tennessee.

BUSING, W. R., MARTIN, K. O. & LEVY, H. (1964). *ORFFE.* Report ORNL-TM-306, Oak Ridge National Laboratory, Oak Ridge, Tennessee.

CHEN, B. M. L. & TULINSKY, A. (1972). *J. Amer. Chem. Soc.* **94**, 4144–4151.

CODDING, P. W. & TULINSKY, A. (1972). *J. Amer. Chem. Soc.* **94**, 4151–4157.

COLLINS, D. M. & HOARD, J. L. (1970). *J. Amer. Chem. Soc.* **92**, 3761–3731.

COLLINS, D. M., SCHEIDT, W. R. & HOARD, J. L. (1972). *J. Amer. Chem. Soc.* **94**, 6689–6696.

CROMER, D. T. (1973). *International Tables for X-ray Crystallography.* Vol. IV, in preparation.

CULLEN, D. L. & MEYER, E. F. JR (1971a). *Chem. Commun.* pp. 616–617.

CULLEN, D. L. & MEYER, E. F. JR (1971b). *Abstr. Amer. Cryst. Assoc.* Summer Meeting, Ames, Iowa, Paper K 15.

CULLEN, D. L. & MEYER, E. F. JR (1973). *Abstr. Amer. Cryst. Assoc.* Winter Meeting, Gainesville, Florida, Paper A1.

FRIEDEL, M. K., HOSKINS, B. F., MARTIN, R. L. & MASON, S. A. (1970). *Chem. Commun.* pp. 400–401.

HAMOR, M. J., HAMOR, T. A. & HOARD, J. L. (1964). *J. Amer. Chem. Soc.* **86**, 1938–1942.

HOARD, J. L. (1972). *Ann. N.Y. Acad. Sci.* In the press.

HOUSTY, J. & CLASTRE, J. (1957). *Acta Cryst.* **10**, 695–698.

International Tables for X-ray Crystallography (1962). Vol. III, p. 215. Birmingham: Kynoch Press.

International Tables for X-ray Crystallography (1973). In preparation.

JOHNSON, C. K. (1965). *ORTEP.* Report ORNL-3794 Revised, Oak Ridge National Laboratory, Oak Ridge, Tennessee.

LAUHER, J. W. & IBERS, J. A. (1973). *J. Amer. Chem. Soc.* **95**, 5148–5152.

MEYER, E. F. JR (1972). *Acta Cryst.* B**28**, 2162–2167.

MEYER, E. F. JR (1973). *J. Appl. Cryst.* **6**, 45.

MORIMOTO, C. N. & MEYER, E. F. JR (1973). *Abstr. Amer. Cryst. Assoc.* Winter Meeting, Gainesville, Florida, Paper F6.

O'ROURKE, M. & CURRAN, C. (1970). *J. Amer. Chem. Soc.* **92**, 1501–1506.

RODGERS, D. & OSBORN, R. S. (1971). *Chem. Commun.* pp. 840–841.

SILVERS, S. J. & TULINSKY, A. (1967). *J. Amer. Chem. Soc.* **89**, 3331–3337.

WILLOUGHBY, T. V. & MEYER, E. F. JR (1973). *Abstr. Amer. Cryst. Assoc.* Winter Meeting, Gainesville, Florida Paper F5.